Development of a Twisted String Actuator-based Exoskeleton for Hip Joint Assistance in Lifting Tasks

Hyeon-Seok Seong[1], Do-Hyeong Kim[1], Igor Gaponov[2] and Jee-Hwan Ryu[1]

Abstract— This paper presents a study on a compliant cable-driven exoskeleton for hip assistance in lifting tasks that is aimed at preventing low-back pain and injuries in the vocational setting. In the proposed concept, we used twisted string actuator (TSA) to design a light-weight and powerful exoskeleton that benefits from inherent TSA advantages. We have noted that nonlinear nature of twisted strings' transmission ratio (decreasing with twisting) closely matched typical torque-speed requirements for hip assistance during lifting tasks and tried to use this fact in the exoskeleton design and motor selection. Hip-joint torque and speed required to lift a 10-kg load from stoop to stand were calculated, which gave us a baseline that we used to design and manufacture a practical exoskeleton prototype. Preliminary experimental trials demonstrated that the proposed device was capable of generating required torque and speed at the hip joint while weighing under 6 kg, including battery.

I. INTRODUCTION

Various studies have reported that a large proportion of workers who have to often perform heavy lifting tasks in industrial and manufacturing settings suffer from lower back pain or related injuries [1], which leads to significant losses to the economy [2]. Over 40% of industrial workers face heavy load lifting tasks at their workplaces [2], and more than 20% of them at some point had to consult specialists to treat short-term or long-term lower back injuries [1]. The main source of these injuries and pains is the combination of lifting and workers' movement with heavy loads, and the resulting injuries are not only difficult to recover from but also have high risk of relapse, even after successful treatment [3] because the workers remain continuous exposure to the same environments and tasks.

Many exoskeletons have been developed to assist industrial workers and decrease their fatigue in order to prevent potential musculoskeletal disorders during heavy object lifting, palletizing, and overhead assembly, among others [2]. One particular type of exoskeletons that has gained significant research attention in recent years is hip and back support exoskeleton. With their simplicity and effectiveness, it became very attractive in various industrial settings. To date, several commercial and experimental exoskeletons for hip and back support have been reported. In most of them, electric motor is directly connected to the hip joint through conventional gear reduction mechanism, like a harmonic drive, to generate comparatively high torques required for lifting while keeping the actuator as light and compact as

[1]Department of Civil and Environmental Engineering, KAIST, Daejeon, South Korea. {hysk.seong, dohyeong, jhryu}@kaist.ac.kr
[2]Institute of Robotics and Computer Vision, Innopolis University, Innopolis, Russia. i.gaponov@innopolis.ru
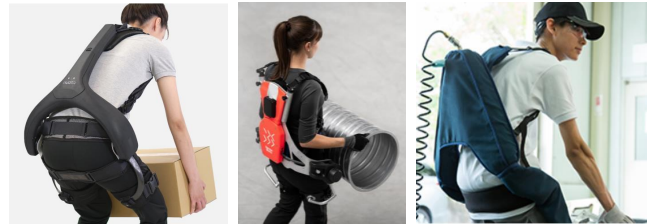
Fig. 1. Various exoskeleton systems for back support. ATOUN Model Y (left), GermanBionic CRAY X (middle), and INNOPHYS Muscle Suit (right)

possible [4], [5], [6], [7]. However, high gear reduction often comes at the cost of low back-drivability and decreased user safety. As an alternative to geared motors, pneumatic and hydraulic actuators have been also extensively used in exoskeleton development [8], [9], [10]. However, they can quickly become too heavy and bulky if the power source (compressor or pump) has to be mounted on the exoskeleton frame itself. Alternatively, placing all the infrastructure that is required for proper actuator operation outside limits laborer's working area and introduces undesired external tethers which may interfere with operations and cause discomfort. Therefore, proper selection of actuator and transmission system plays an essential role in exoskeleton design.

Twisted string actuator (TSA) is an emerging type of cable actuator that has attracted significant research attention in the past decade. In TSA, a string twisted by a motor contracts and thus acts as a rotary-to-linear transmission. Applications of TSAs range from robotic hands and mobile robots to lightweight assistance devices and exoskeletons [11]. Advantages of TSA include light weight, mechanical simplicity, high transmission ratios, and low inertia. However, this comes at the cost of nonlinearity in the gear ratio, which is high initially but can decrease significantly with twisting.

This paper outlines design and experimental investigation of a novel TSA-based exoskeleton for lower back assistance. We have designed the device to take advantage of the variable nature of the transmission ratio of twisted strings (high when untwisted and decreasing with twisting) which fits the joint torque profile required for load lifting from stoop to stand. The mechanical components and joints of the power suit were designed accordingly, which helped us reduce the weight of the device by selecting compact gearless motor.

To the best of our knowledge, this is the first exoskeleton based on TSA whose mechanical design takes into account

nonlinear properties of twisted strings. We are only aware of a single study on TSA-based power suit for lower back assistance, however, in it the authors have implemented TSA in the exoskeleton in the capacity of linear actuator and have not optimized actuator size or hardware structure of the device by taking into account TSA characteristics [12].

This paper presents a systematic way to design hip-joint exoskeleton based on the TSA. Firstly, we calculated actuator stroke and torque at the hip joint required for lifting a hand-held 10-kg load from stoop to stand position based on a simplified kinematics of the human body. Next, we designed an anthropomorphic mechanism for assistance in which strings were placed along the wearer's back. Finally, we have manufactured the device and evaluated its performance experimentally. The proposed device was able to satisfy torque and speed requirements while weighing under 6 kg, including the battery.

II. MATHEMATICAL MODELING
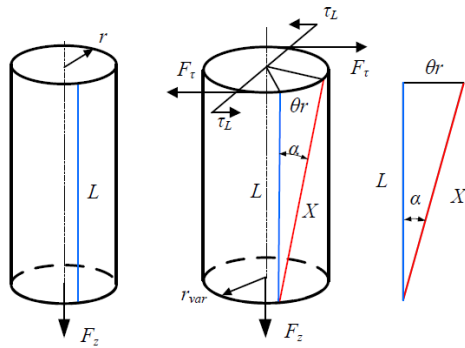
A. Twisted String Model

Fig. 2. A schematic diagram of a section of twisted string

Mathematical modeling of twisted strings has been studied extensively by various research groups [13], [14], [15]. The simplest model can be derived by assuming the twisted string to be a cylinder, as depicted in Fig.2. When the line of initial length L and radius r is twisted for an angle θ, its contracted length becomes X, and these quantities can be related through the geometry of unwound cylinder as follows:

$$L = \sqrt{X^2 + \theta^2 r^2} \qquad (1)$$

The resulting contraction of the string $\Delta X = L - X$ can be thus found as

$$\Delta X = L - \sqrt{L^2 - \theta^2 r^2} \qquad (2)$$

The conventional mathematical model (2) is based on the assumption that the string is a homogeneous cylinder composed of many fibers whose compression by the surrounding fibers is negligibly small, with no air gaps between them.

B. Calculation of Required Exoskeleton Torque

The main purpose of the proposed hip-joint exoskeleton was providing additional assistance to the wearer during lifting of heavy load to reduce muscle fatigue. To design the
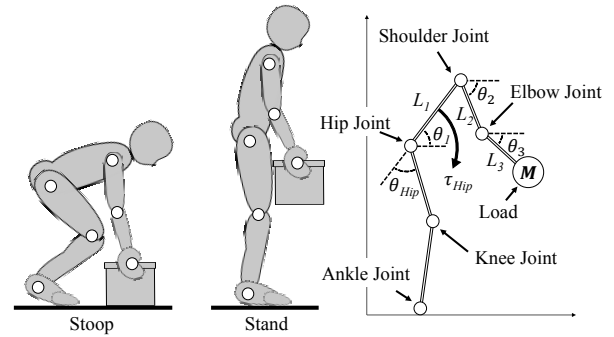

Fig. 3. Kinematic model of the human body in sagittal plane during load lifting tasks: Schematic representation of limbs and joints (left) and the corresponding kinematic chain (right)

exoskeleton appropriately, we firstly needed to find the range of hip joint torques required for lifting the target payload of 10 kg [16], [17]. All the calculations were carried out based on a simplified kinematic representation of the human body in the sagittal plane depicted in Fig. 3, with the load located between the forearms (hands) and assuming that the wearer has to perform stoop-to-stand motion during the lifting. The variables $L_1 - L_3$ and $\theta_1 - \theta_3$ denote the lengths and joint angles of trunk, upper arm and lower arm, respectively, θ_{Hip} denotes the angle between hips and the trunk, and M corresponds to the load's mass. The hip joint torque τ_{Hip} caused by the payload can be therefore calculated as follows:

$$\tau_{hip} = Mg(L_1 \cos\theta_1 + L_2 \cos\theta_2 + L_3 \cos\theta_3) \qquad (3)$$

The lengths L_1, L_2 and L_3 were selected to be 0.6 m, 0.25 m and 0.3 m, respectively, based on anthropometric study [18]. Please note that the body and limbs' weights have not been considered in the calculation since we were targeting compensation for the payload's weight during lifting, not the body weight.
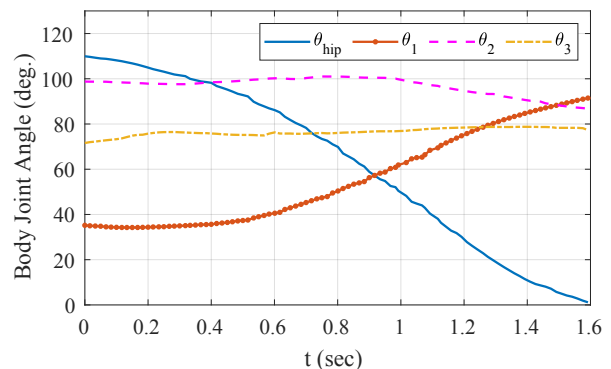

Fig. 4. Temporal plots of joint angles during lifting: Trunk (θ_1), shoulder (θ_2), elbow (θ_3) and hip (θ_{hip})

The torque (3) generated by the payload requires the joint angles measurement during lifting. To obtain these data, we have performed experiments and recorded the joint angle values (θ_{hip}, θ_1, θ_2, θ_3) during lifting of a 10-kg object.

Data were acquired with the help of 'Perception Neuron V1' motion capture system [19], and Fig. 4 shows time history of joint angles when the human moved from stoop to stand in just over 1.5 seconds of time. One can note that, while standing, the hip angle θ_{hip} is approximately zero, while the other angles $\theta_1 - \theta_3$ converge to $\pm 90°$.
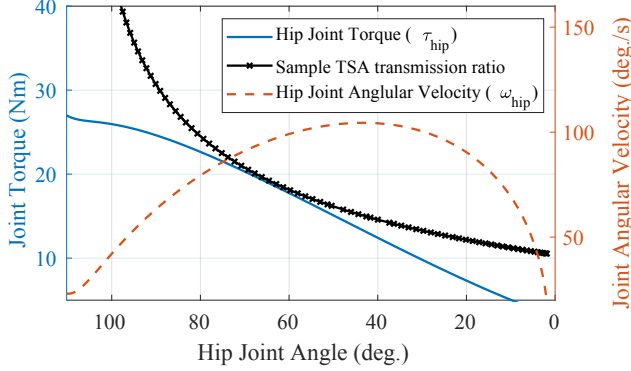

Fig. 5. Required hip joint torque and angular velocity when lifting a 10-kg load

After obtaining these data, one can calculate hip joint torque τ_{hip} and angular velocity ω_{hip} required during lifting as functions of the hip-joint angle θ_{hip}, as shown in Fig. 5. One can note that, in the beginning of the stoop-to-stand motion, comparatively large torque is required, with its values gradually decreasing during motion [17]. It is worth pointing out this torque profile closely matches the shape of TSA transmission ratio during twisting, which is initially high for untwisted strings and then drops with twisting. Therefore, TSA can fit the application well if designed properly, and the corresponding design outline is given in the following section.

III. EXOSKELETON DESIGN CONCEPT AND CONSIDERATIONS

A. Design Concept

To achieve desired hip-joint torque and angular velocity profiles with the support of TSA, one must consider both hip-joint mechanism design and kinematic structure of the exoskeleton itself, as well as string routing. In this research, we opted to go with the most straightforward mechanism solution for to make the device as compact and light-weight as possible. In the proposed device, the string is routed along the wearer's back to the hip-joint, as shown in Fig. 6. The rotational joint connects two rigid links, trunk and hip, that are interfaced with corresponding body parts via flexible harness. The string is wrapped around a pulley located at the hip joint in such a way that linear contraction of the string generates torque on the pulley that is then transmitted to the hip.

With this concept in mind, we moved on to study the emerging kinematics and statics relationships of the proposed mechanism.
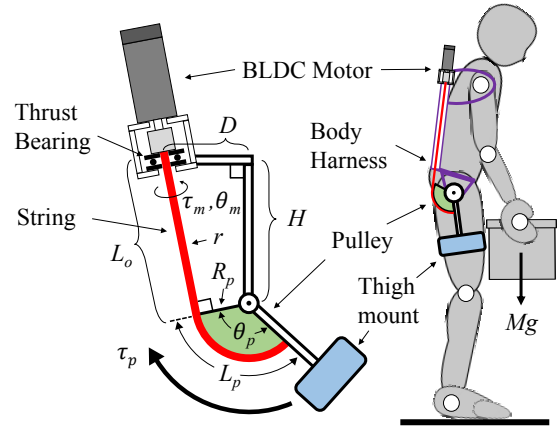

Fig. 6. Simplified kinematic structure of the hip joint Exoskeleton

B. Analysis of Exoskeleton Kinematics

To study the kinematics of the exoskeleton, we used a simplified scheme depicted in the main variables to consider are the length of trunk coupled link H, the offset between the end point of trunk coupled link and motor installation point on the upper back D, pulley (cam) radius R_p, and the hip joint angle θ_p.

Once these parameters are given, the length of the string until the pulley L_o, which starts from the top of the back to top of the pulley of the hip joint, can be obtained with the following formula:

$$L_o = \sqrt{D^2 + H^2 - R_p^2} \tag{4}$$

The length of the string wrapped around the pulley L_p can be found for known radius R_p and maximum rotation angle θ_p^{max} as $L_p = R_p \theta_p^{max}$. The maximal value of θ_p^{max} was obtained from the motion capture data θ_{hip} and was equal to $108°$. As the result, the total string length L can be simply calculated by summing L_o and L_p:

$$L = L_o + L_p \tag{5}$$

One of the key design parameters of the proposed exoskeleton is the pulley radius R_p, since it determines TSA stroke and affects the torque generated by the actuator at the hip joint. Assuming the maximum contraction of the string relative to its untwisted length to be given by p, the upper boundary on the pulley radius can be calculated as follows:

$$R_p \leq pL / \theta_p^{max} \tag{6}$$

At the same time, assuming that the tension on the strings can be calculated with a simple cam equation $F_s = \tau_{hip}/R_p$, one can calculate the lower bound of R_p from the standpoint of cable strength for known maximal torque and tensile strength:

$$\frac{\tau_{hip}^{max}}{F_s^{max}} \leq R_p \tag{7}$$

Now, substituting parameters D and H shown in Fig. 6 into (6) one obtains both constraints on the pulley radius:

$$\frac{\tau_{hip}^{max}}{F_s^{max}} \leq R_p \leq \sqrt{\frac{D^2 + H^2}{\left(\frac{1-p}{p} \cdot \theta_p^{max}\right)^2 + 1}} \qquad (8)$$

To determine the minimum pulley radius R_p using (8), we used the value of F_s^{max} = 2300 N, which is double the maximum tensile strength of the string we used (1 mm line diameter, LIROS Dyneema Braid [20]) since 2 strings were used in parallel in the TSA. As the result, pulley radius R_p must be over 12 mm to satisfy the cable strength condition. As for the upper bound of R_p, the value of p is commonly selected to be 30% to avoid over-twisting which shortens the string lifetime and causes unstable contraction behavior [21]. Thus, for selected parameter values $D = 120$ mm and $H = 490$ mm, the maximum pulley radius calculated with (8) is $R_p^{max} = 111$ mm. This suggests that the strings' length L can be anywhere between 526 and 702 mm, as suggested by (4) and (5).

C. Calculation of TSA Torque

Assuming the twisted string to be rotary-to-linear transmission, we can write the pulling force F_s it generates when twisted by motor torque τ_m as

$$F_s = G_{TSA}\tau_m \qquad (9)$$

where G_{TSA} $[m^{-1}]$ is the transmission ratio of twisted string and can be found as the ratio between input and output velocities by differentiating (2). Thus, assuming the angle of twisting to be denoted by θ_m, one obtains

$$G_{TSA} = \frac{\frac{d}{dt}\theta_m}{\frac{d}{dt}\triangle X} = \frac{\sqrt{L^2 - (r\theta_m)^2}}{r^2 \theta_m} = \frac{L - \triangle X}{r\sqrt{\triangle X(2L - \triangle X)}} \qquad (10)$$

One can note that the TSA transmission ratio given by (10) is nonlinear and, while originally high, decreases with twisting.

Knowing that TSA stroke is converted into the motion of the pulley as $\triangle X = R_p(\theta_p^{max} - \theta_p)$, one can substitute this into the right-hand side of (10) and after some simplifications obtained

$$G_{TSA} = \frac{L/(R_p(\theta_p^{max} - \theta_p)) - 1}{r\sqrt{2L/(R_p(\theta_p^{max} - \theta_p)) - 1}} \qquad (11)$$

Assuming that the created force (tension) on the string F_s is converted into pulley torque τ_p with non-ideal transmission efficiency η, one can find τ_p as follows:

$$\tau_p = \eta R_p G_{TSA}\tau_m \qquad (12)$$

Thus, the pulley torque is determined by the transmission efficiency, pulley radius, transmission ratio and motor torque.

Finally, the total mechanism transmission ratio between the pulley and motor torques can be found from (12) as follows:

$$G(R_p, \theta_p) = \tau_p/\eta\tau_m = R_p G_{TSA} \qquad (13)$$

To completely compensate for the payload, the exoskeleton must be able to generate pulley torque τ_p exceeding the

required hip joint torque τ_{hip} for the whole range of motion θ_p:

$$\tau_p = \eta G\tau_m \geq \tau_{hip} \qquad (14)$$

With the same principle, one can find pulley radius R_p to satisfy requirements on joint velocity ω_p for given motor speed ω_m as

$$\omega_p = \frac{\omega_m}{G} \geq \omega_{hip} \qquad (15)$$

$$\frac{1}{\eta}\frac{\tau_{hip}}{\tau_m} \leq G \leq \frac{\omega_m}{\omega_{hip}} \qquad (16)$$

As the result, motor torque τ_m, angular velocity ω_m and pulley radius R_p can be taken into account to ensure that the transmission ratio G of the design mechanism satisfies both constraints in (16).
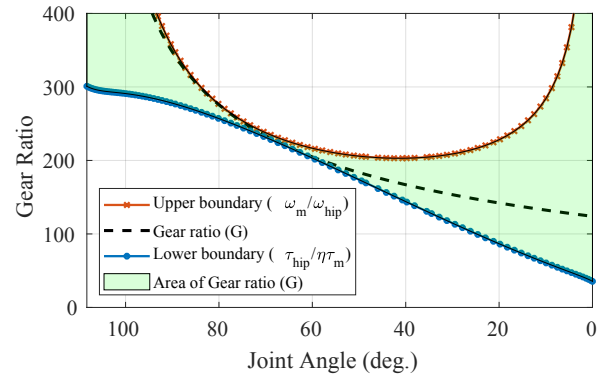

Fig. 7. Desired transmission ratio of the exoskeleton

Fig. 7 illustrates the desired transmission ratio profile with respect to the hip joint angle for a conservative estimate of $\eta = 0.623$. The lower boundary is given by the motor torque required to satisfy task requirements, whereas the upper bound is given by the ratio between motor velocity and desired angular velocity of the hip joint.

If the mechanism transmission ratio is designed to be too low (crossing the lower boundary at some point), the system will not be able to generate enough torque throughout the whole range of motion. Conversely, if the transmission ratio is selected to be too high, the system will be excessively powerful and too slow. As the pulley radius R_p increases, the transmission ratio of the proposed mechanism given by (13) shifts up, and if the nominal motor torque and velocity are known, tuning parameter R_p can help ensure that the resulting transmission ratio is located within design bounds.

TABLE I

MECHANISM, STRING, AND MOTOR PARAMETERS

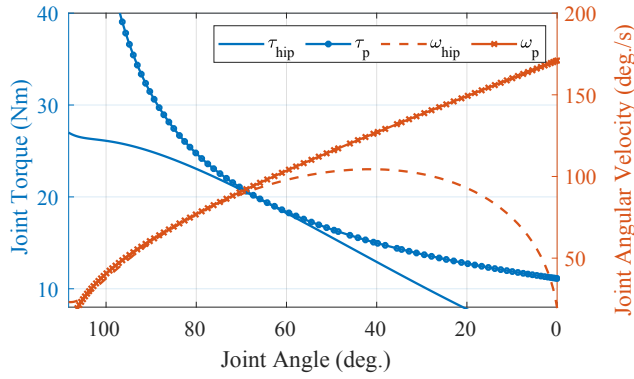| D (mm)	H (mm)	L (mm)	r (mm)
120	490	623	0.7
R_p (mm)	η	τ_m (Nm)	ω_m (rad/s)
65	0.623	0.144	370

Fig. 8.   Achievable hip-joint torque and speed with selected design parameters

Fig. 8 shows theoretical torque and velocity characteristics that the mechanism provides with design parameters given in Table I. One can see that both produced torque τ_p and speed ω_p satisfy the requirements with the selected pulley of radius $R_p = 65$ mm and nominal motor torque and speed of $\tau_m = 0.144$ Nm and $\omega_m = 370$ rad/s, respectively.
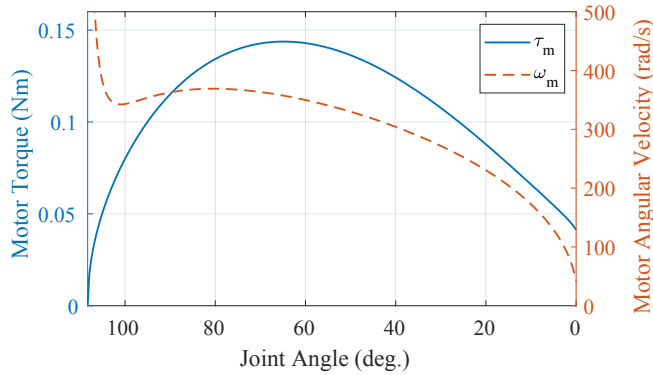

Fig. 9.   Required TSA motor torque and speed

Fig. 9 shows calculated TSA motor torque τ_m and speed ω_m that are required to satisfy hip-joint torque and speed specifications during lifting 10 kg load. One can note that, according to the mathematical model, peak motor torque and speed were approximately 0.15 Nm and 370 rad/sec, respectively, suggesting that an electric motor with rated power of 55 W or above should theoretically satisfy application requirements. Once all required calculations are completed, we proceed with manufacturing and experimental evaluation of the proposed exoskeleton.

IV. EXPERIMENTAL EVALUATION OF THE EXOSKELETON

A. Hardware Prototype

A prototype TSA-based hip joint exoskeleton has been designed according to the guidelines described in the previous section and is shown in Fig. 10, and a close-up of the pulley assembly is depicted in Fig. 11.

The prototype is composed of two identical actuation mechanisms mounted symmetrically on a compliant body
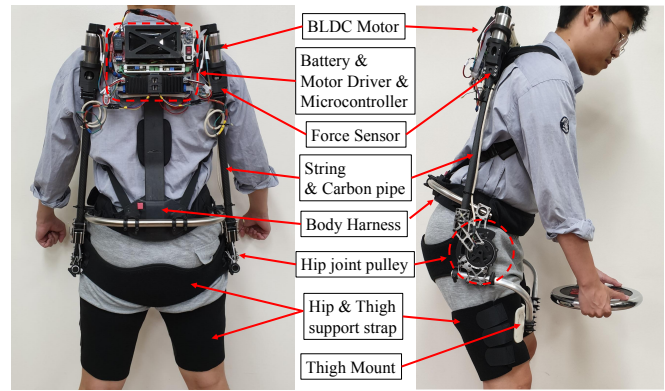

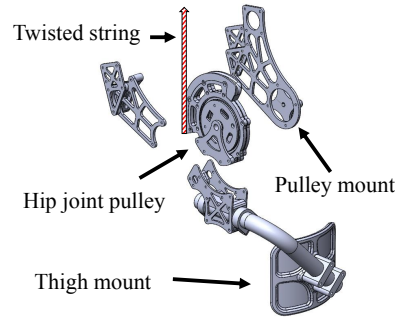Fig. 10.   Prototype of TSA-based hip joint exoskeleton

Fig. 11.   Exploded view of the hip joint pulley

harness. Each half of the exoskeleton features a thigh mount to support joint pulley, a BLDC motor (Maxon 24V 170W EC40 with a 2000-CPT encoder without gear), motor driver (ESCON Module 50/8 HE), an 4096-CPT absolute optical encoder (AMT 203-V) measuring the hip joint pulley rotation angle, hollow-type loadcell (Futek LTH300) installed at the motor side and capable of measuring up to 110 kg compression force, and 2 Dyneema strings (LIROS) used in parallel. A 96-Mhz ARM-type micro-controller (Teensy 3.2) runs control and data acquisition software.

The strings were guided inside hollow carbon pipes and connected to the motor shaft coupling on one end and to the hip joint pulley on the other. The strings were aligned with the rotation axis of the motor. The total weight of the system including battery was measured to be 6 kg.

Having manufactured this device, we proceeded to its experimental evaluation.

B. Performance Evaluation

In the designed experimental scenario, the wearer was asked to perform stoop-to-stand motion 5 times while holding a 10-kg load in their hands. Temporal plots of required and experimental pulley torques and speeds are shown in Fig. 12 and Fig. 13, respectively. The measured curves in the plots correspond to the average values based on several motion cycles, while the greyed-out areas correspond to variables' variations between trials. One can note that the proposed exoskeleton comfortably achieves required specifications outlined in Section. II-B for lifting a 10-kg load.
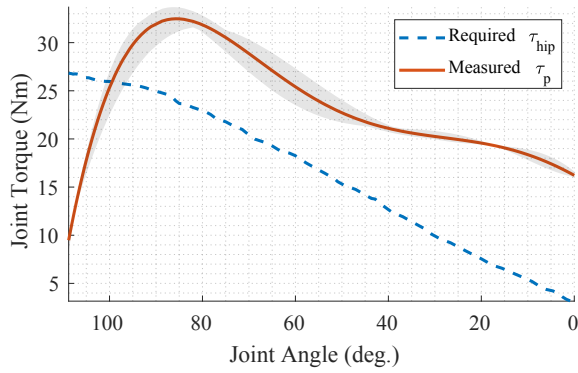
Fig. 12. Torque generated on the hip joint by the proposed TSA-based exoskeleton
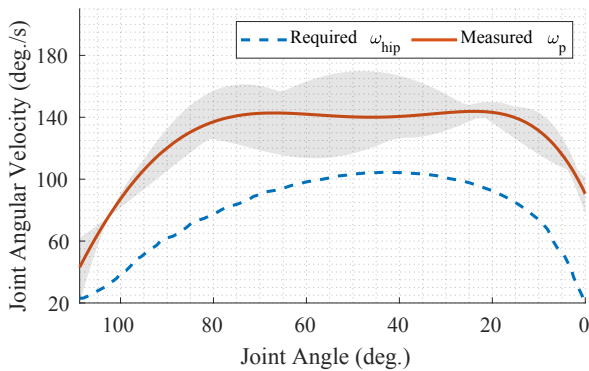

Fig. 13. Angular velocity of the hip joint in the proposed exoskeleton

During the trials, we observed that initially, measured torque is less than the required one, which is most likely caused by non-negligible compliance of the string and flexibility. As the result, while the string is being twisted by the motor, the force produced by the TSA is originally spent on harness deformation rather than on torque generation. Once all soft and compliant components of the exoskeleton are pre-tensioned, TSA operates as desired. As for the joint speed, since the exoskeleton is capable of moving faster than expected, the speed can be adjusted by control system tuning.

V. Discussion and Conclusion

This paper presents design guidelines and experimental evaluation of a TSA-based exoskeleton for hip assistance during lifting tasks. The device takes advantage of the nonlinear nature of TSA transmission ratio and aims at using it effectively to design a powerful and compact active exoskeleton. We carried out kinematics and statics analysis of the proposed device based on task requirements from anthropometric data, and used the results for optimal mechanism design and actuator selection. We have manufactured a practical exoskeleton prototype based on the outlined design specifications, and verified experimentally that the proposed device can meet torque and speed requirements for the hip joint when assisting the wearer in lifting a 10-kg payload.

In the nearest future, we are planning to conduct a more thorough experimental evaluation and verification of the exoskeleton's performance via a cohort study. We are also looking into development of intuitive human-machine interface so that the wearer can adjust motion range and speed in real time. Lastly, we would like to conduct a longitudinal study on lifetime of twisted string in the proposed system and look into ways of expanding it.

References

[1] M. Ghaffari, A. Alipour, I. Jensen, A. A. Farshad, and E. Vingard, "Low back pain among iranian industrial workers," *Occupational Medicine*, vol. 56, no. 7, pp. 455–460, 2006.
[2] M. P. De Looze, T. Bosch, F. Krause, K. S. Stadler, and L. W. OSullivan, "Exoskeletons for industrial application and their potential effects on physical work load," *Ergonomics*, vol. 59, no. 5, pp. 671–681, 2016.
[3] I. Budihardjo, "Studies of compressive forces on l5/s1 during dynamic manual lifting," 2002.
[4] H. Yu, I. S. Choi, K.-L. Han, J. Y. Choi, G. Chung, and J. Suh, "Development of a stand-alone powered exoskeleton robot suit in steel manufacturing," *ISIJ International*, vol. 55, no. 12, pp. 2609–2617, 2015.
[5] S. Toxiri, J. Ortiz, J. Masood, J. Fernández, L. A. Mateos, and D. G. Caldwell, "A powered low-back exoskeleton for industrial handling: considerations on controls," in *Wearable Robotics: Challenges and Trends*. Springer, 2017, pp. 287–291.
[6] ATOUN, "Atoun model y," http://atoun.co.jp/products/atoun-model-y.
[7] GermanBionic, "Cray x," https://www.germanbionic.com/en/crayx/.
[8] A. B. Zoss, H. Kazerooni, and A. Chu, "Biomechanical design of the berkeley lower extremity exoskeleton (bleex)," *IEEE/ASME Transactions on Mechatronics*, vol. 11, no. 2, pp. 128–138, April 2006.
[9] N. Tsagarakis, D. Caldwell, and G. Medrano-Cerda, "A 7 dof pneumatic muscle actuator (pma) powered exoskeleton," in *8th IEEE International Workshop on Robot and Human Interaction. RO-MAN'99 (Cat. No. 99TH8483)*. IEEE, 1999, pp. 327–333.
[10] INNOPHYS, "Musclesuitpower," https://innophys.jp/en/product/power/.
[11] J. Zhang, J. Sheng, C. T. ONeill, C. J. Walsh, R. J. Wood, J. H. Ryu, J. P. Desai, and M. C. Yip, "Robotic artificial muscles: Current progress and future perspectives," *IEEE Transactions on Robotics*, 2019.
[12] Z. Yao, C. Linnenberg, R. Weidner, and J. Wulfsberg, "Development of a soft power suit for lower back assistance*," in *2019 International Conference on Robotics and Automation (ICRA)*, May 2019, pp. 5103–5109.
[13] I. Godler, K. Hashiguchi, and T. Sonoda, "Robotic finger with coupled joints: A prototype and its inverse kinematics," in *2010 11th IEEE International Workshop on Advanced Motion Control (AMC)*. IEEE, 2010, pp. 337–342.
[14] G. Palli, C. Natale, C. May, C. Melchiorri, and T. Wurtz, "Modeling and control of the twisted string actuation system," *IEEE/ASME Transactions on Mechatronics*, vol. 18, no. 2, pp. 664–673, April 2013.
[15] I. Gaponov, D. Popov, and J.-H. Ryu, "Twisted string actuation systems: A study of the mathematical model and a comparison of twisted strings," *IEEE/ASME Transactions on Mechatronics*, vol. 19, no. 4, pp. 1331–1342, 2013.
[16] S. H. Snook, C. Irvine, and S. Bass, "Maximum weights and work loads acceptable to male industrial workers," *American Industrial Hygiene Association Journal*, vol. 31, no. 5, pp. 579–586, 1970.
[17] S. Hwang, Y. Kim, and Y. Kim, "Lower extremity joint kinetics and lumbar curvature during squat and stoop lifting," *BMC musculoskeletal disorders*, vol. 10, no. 1, p. 15, 2009.
[18] N. I. A. Rahman, S. Z. M. Dawal, N. Yusoff, and N. S. M. Kamil, "Anthropometric measurements among four asian countries in designing sitting and standing workstations," *Sādhanā*, 2018.

[19] J. Chen, J. Qiu, and C. Ahn, "Construction worker's awkward posture recognition through supervised motion tensor decomposition," *Automation in Construction*, vol. 77, pp. 67–81, 2017.

[20] L. GmbH, "Dyneema braid," https://www.liros.com/.

[21] M. Tavakoli, R. Batista, and P. Neto, "A compact two-phase twisted string actuation system: Modeling and validation," *Mechanism and Machine Theory*, vol. 101, pp. 23–35, 2016.